Published in final edited form as:
Life Sci. 2008 October 24; 83(17-18): 581–588. doi:10.1016/j.lfs.2008.08.011.

Effects of oral consumption of the green tea polyphenol EGCG in a murine model for human Sjogren's syndrome, an autoimmune disease

Kevin Gillespie, DMD[*], **Isamu Kodani, MD, PhD**[*], **Douglas P. Dickinson, PhD**, **Kalu U.E. Ogbureke, MD, PhD**, **Amy M. Camba, BS**, **Mengjie Wu, DMD, PhD**, **Stephen Looney, PhD**, **Tin-Chun Chu**, **Haiyan Qin, MS**, **Frederick Bisch, DMD**, **Mohamed Sharawy, PhD**, **George S. Schuster, DDS, PhD**, and **Stephen D. De Hsu, PhD**

Department of Oral Biology, School of Dentistry, Medical College of Georgia, Department of Periodontology, US Army Fort Gordon, Fort Gordon, GA. K.G., F.B., Department of Oral and Maxillofacial Surgery, Totorri University Hospital, Faculty of Medicine, Tottori University, Yonago, Japan. I.K., School of Dentistry, Hospital of Stomotology, Zhejiang University, Hangzhou, China. M.W., Department of Oral Biology, School of Dentistry, Medical College of Georgia, Augusta, GA USA. S.D.H., D.P.D., H.Q., K.U.E.O., A.M.C., S.L., M.S., G.S.S., Department of Biological Sciences, the College of Arts and Science, Seton Hall University. T.C.

Abstract

Protection of glandular acinar cells from autoimmune-induced damage would be of significant clinical benefit to Sjogren's syndrome (SS) patients. EGCG (the most abundant green tea polyphenol) possesses anti-apoptotic, anti-inflammatory, and autoantigen-inhibitory properties. To investigate if EGCG can protect against certain autoimmune-induced pathological changes in the salivary glands of the non-obese diabetic (NOD) mouse model for SS-like symptoms, animals were provided with either water or water containing 0.2% EGCG. At the age of 8, 16 and 22 weeks, samples were collected for pathological and serological analysis. Massive lymphocyte infiltration was observed in the salivary glands of the water-fed group at the age of 16 weeks, while the EGCG group showed significantly reduced lymphocyte infiltration. By 22 weeks of age, animals fed with water demonstrated elevated levels of apoptotic activity within the lymphocytic infiltrates, and high levels of serum total anti-nuclear antibody, in comparison with the animals fed with EGCG. Remarkably, proliferating cell nuclear antigen (PCNA) and Ki-67 levels in the salivary glands of NOD animals fed with water were significantly elevated in comparison to BALB/c control mice; in contrast, PCNA and Ki-67 levels in EGCG-fed NOD animals were similar to BALB/c controls. These results indicate that EGCG is able to protect the NOD mouse submandibular glands from autoimmune-induced inflammation, and reduces serum autoantibody levels. Abnormal proliferation, rather than apoptosis, appears to be a characteristic of the NOD mouse gland that is normalized by EGCG. The evidence suggests that EGCG could ultimately be used to delay or manage SS-like autoimmune disorders.

Keywords

Green tea polyphenol; EGCG; Sjogren's syndrome; NOD mouse; Autoimmune

Corresponding author: Stephen Hsu, Department of Oral Biology, AD1443 School of Dentistry, Medical College of Georgia, Augusta, GA 30912-1126 USA, Tel: 706-721-2317, Fax: 706-721-3392, E-mail: shsu@mail.mcg.edu.
[*]Authors with equal contribution.
Request for reprint should be addressed to Stephen Hsu, Department of Oral Biology, AD1443 School of Dentistry, Medical College of Georgia, Augusta, GA 30912-1126 USA, Tel: 706-721-2317, Fax: 706-721-3392, shsu@mail.mcg.edu

Introduction

Autoimmune disorders, the third most common group of diseases in the United States, affect about 8% of the population. The pathogenesis of SS, a relatively common autoimmune disease, is poorly understood. Primary SS is characterized by inflammatory infiltration of the lacrimal and salivary glands, leading to loss of secretory function and resulting ocular and oral health problems. Environmental and genetic factors appear to contribute to the etiology (Bolstad and Jonsson, 2002; Yamamoto, 2003; Sawalha et al., 2003). T-cell-mediated cytotoxicity and autoantibodies are important in loss of gland function (Rehman, 2003; Manganelli and Fietta, 2003; Hayashi et al., 2003; Hayashi et al., 2004). Glandular epithelial cells also contribute to the autoimmune process by secreting pro-inflammatory cytokines. The trigger(s) for the autoimmune attack on exocrine cells are unknown. One mechanism may involve aberrant expression and translocation of nuclear autoantigens onto the acinar cell membrane during apoptosis, where they are exposed to antigen-presenting cells such as macrophages and dendritic cells (Manganelli and Fietta, 2003; Cravens and Lipsky, 2002; van Woerkom, 2004). During apoptosis, autoantigens redistribute in acinar cells to form apoptotic bodies and blebs, where autoantigen proteins, including SS-A/Ro, SS-B/La, Ku, PARP, fodrin, golgins and NuMA, are clustered as subcellular structures. Structural changes in auto-antigens may contribute to an altered configuration of the autoantigen cluster, leading to the autoimmune response (Rosen and Casciola-Rosen, 2004). Therefore, acinar cells likely play a key role in initiating and sustaining this autoimmune disorder.

The NOD mouse strains (e.g. NOD/Lt, NOD.B10-H2b, NOD-scid) comprise an important model system that has provided clues to the cellular mechanisms involved in SS (Cha et al., 2002;Jonsson et al., 2006). During the past two years, almost 50% of published animal studies for SS used this model. It was originally used as a model for type I diabetes. However, the NOD/Lt strain develops a lymphocytic infiltration of exocrine tissues at 10–12 weeks of age, particularly in females, and progresses to a dramatic reduction in saliva secretion. It has been suggested that early changes in glandular homeostasis involving apoptosis contribute to disease progression (Humphreys-Beher et al., 1998). Data from studies in the NOD mouse and human SS patients are consistent with a model for SS in which there is an initial phase during which dysregulation of glandular homeostasis triggers the disease, followed by an immune cell-mediated phase that leads to a loss of secretory function (Cha et al., 2002). Collectively, these observations suggest that three potential strategies for ameliorating SS by directly targeting the acinar cells could be selective inhibition of their apoptosis, autoantigen expression, and production of pro-inflammatory cytokines.

Currently, there is no known cure for SS, nor is there knowledge for prevention or delay of such disease. Treatment of the symptoms is generally relies on artificial lubricants as saliva or tear substitutes (Baudouin et al., 2004). Recently, FDA-approved agents, such as pilocarpine and cevimeline, are used as salivary stimulants to treat xerostomia (Fox, 2003; Cassolato and Turnbull, 2003;Porter et al., 2003), as well as interferon γ (IFN-γ) (Khurshudian, 2003). It was suggested that gene therapy might be one of the future treatments for primary SS by inducing the growth and differentiation of glands (Fox, 2004). In addition, plant extracts and Chinese traditional medicine had been recognized as an option to treat SS and/or xerostomia (Ohno et al., 1990; Zhao et al., 1989). These naturally occurring phytochemicals may serve as an alternative approach to treating SS-associated disorders. One group of compounds with considerable potential is the green tea polyphenols (GTPs), which possess chemopreventive, anti-apoptotic, and anti-inflammatory activities (Mukhtar and Ahmad, 2000, Sueoka et al., 2001, Hsu and Dickinson, 2006). Previously, we showed that NOD mice fed with GTPs had reduced lymphocytic infiltration of the submandibular gland 3 weeks after the onset of diabetes (Hsu et al, 2007). GTPs are extracted from green tea leaves as a complex mixture of polyphenolic compounds. Here, we sought to test if a purified GTP, EGCG, could modulate

SS-like pathological symptoms in the NOD mouse, evaluate the time course of changes, and determine its effects on apoptosis and cell proliferation.

Materials and Methods

Chemicals and Antibodies

EGCG (>95%) was purchased from Sigma-Aldrich (St. Louis, MO). Anti-human PCNA (FL-261) and actin (I-19) goat polyclonal antibody were purchased from Santa Cruz Biotechnology, Santa Cruz, CA. Anti-human Ki-67 antibody was purchased from Abcam Inc, MA. The Mouse Anti-Nuclear Antibodies (ANA) ELISA Kit was purchased from Alpha Diagnostic International, Inc. San Antonio, TX.

Animals

All animal protocols in this study were approved by the Institutional Animal Care and Use Committee. A total of 72 NOD/ShiLtJ (001976, previously designated as NOD/tJ) mice were purchased at the age of 3 weeks from Jackson Laboratory, MN. The animal were maintained in a pathogen-free environment, housed at 5 mice/cage, and fed ad libitum. Two treatment groups of 36 mice per group were randomly assigned. One group was fed with EGCG, the other with water. EGCG exposure (0.1% w/v) was initiated at 4 weeks of age, and the concentration increased to 0.2% w/v at the age of 8 weeks, when the animals reached reproductive age. Water bottles for each cage were filled daily with freshly prepared EGCG-water. The progress of diabetic autoimmune disease was determined by a test of urinary glucose using glucotest strips (Glucotest, Boehringer Mannheim, Mannheim, Germany). Animals testing positive for urinary glucose with this method were labeled as “disease positive” from that day of testing. The body weight of each mouse was monitored and recorded. At the age of week 8, 16 and 22, 12 animals from each treatment group were removed and euthanized by CO_2 inhalation followed by thoracotomy. Blood was collected by cardiac puncture, and the submandibular glands were collected and weighed. Each pair of salivary glands collected was separated into two lobes (free from the sublingual gland). One lobe was fixed in 10% neutral-buffered formalin and paraffin-embedded for pathological and immunohistochemistry analysis. The opposite lobes were stored at −80° C for molecular analysis.

Determination of Serum Total Anti-Nuclear Antibodies

Serum samples were examined by ELISA assay for anti-SS-associated autoantibodies using the Mouse Anti-Nuclear Antibodies (ANA) ELISA Kit (Alpha Diagnostic International, Inc. San Antonio, TX) according to the manufacturer’s instructions, as previously described (Hsu et al, 2007). Briefly, samples in triplicate were analyzed with blanks, positive and negative controls in 96-well plates by ELISA reaction, photodetection using a VERSAmax Microplate Reader at 450nm, and statistical analysis using two-tailed student *t-test*.

Histopathological Analysis

The protocol has been adapted using the recently published cumulative focus score (cFS) criteria, for the assessment of salivary gland inflammatory infiltrates as a component of the diagnosis of SS (Morbini, 2005). Five micron-thick (5 μm) serial sections were cut and stained with hematoxylin and eosin (H&E) for histopathological evaluation. The inflammatory cell infiltrate was determined by a standardized scoring system. The standardized system scores the number of focal inflammatory cell aggregates containing 50 or more lymphocytes in each 4-mm^2 area of a salivary gland. The salivary gland lobules with prominent ductal dilation and/or parenchyma atrophy are excluded from scoring, regardless of the pattern of inflammation, as well as the areas of a gland showing extra vascular polymorphonuclear leukocytes. In

addition, ducts of salivary glands exhibiting various histological changes such as metaplasia, hyperplasia, thinning or oncocytic changes, are noted.

Once the glandular foci were identified, a quantitative analysis of the focal areas was performed by using computer software (BIOQUANT NOVA PRIME 6.75, Bioquant Co., Nashville, TN, U.S.A.). One hematoxylin and eosin (H&E) stained submandibular salivary gland section was selected at random for each animal and images of areas containing foci were loaded into the software. The areas of lymphocyte infiltration foci were captured individually and measured quantitatively using relative density units. The numbers generated from this software represent areas (in arbitrary units) occupied by lymphocytes in the salivary glands.

Immunohistochemical Analysis

Immunohistochemical staining was performed using a standard protocol with Histo-plus Kits (ZYMED Laboratories, CA, U.S.A.) according to the manufacturer's directions. Deparaffinized sections were immersed in methanol containing 3% hydrogen peroxide for 20 min. The sections were incubated with anti PCNA polyclonal antibody (FL-261; Santa Cruz Biotechnology, CA, U.S.A., diluted 1:100) overnight at 4°C or were incubated with anti-Ki-67 polyclonal antibody (Abcam Inc, MA, U.S.A. diluted 1:1500) for 1 hour at room temperature. The sections were then incubated with the biotinylated secondary antibody for 10 min and HRP-streptavidin for 10 min. Peroxidase staining was performed for 3~7 min using a solution of DAB chromogen. The sections were counterstained with 0.5% methyl green.

At least 1000 cells were counted, and the percentage of cells showing positive nuclear staining was designated as the lymphocytic index.

Apoptosis Analysis (TUNEL Assay)

Cells with nuclear DNA fragmentation were visualized by the TUNEL method using the ApopTag Plus Peroxidase in situ apoptosis detection kit (Chemicon International, CA, U.S.A.) according to the manufacturer's directions. Briefly, after deparaffinization, endogenous peroxidase activity was quenched with 3% hydrogen peroxide in PBS for 5 min at room temperature. Then the sections were incubated with terminal deoxynucleotidyl-transferase (TdT) enzyme in a moist chamber for 60 min at 37°C. Incubation with antidigoxigenin-conjugate for 30 min at room temperature was conducted, followed by color development with DAB substrate. Methyl green was used for counterstaining.

TUNEL indices (TI) were defined as the ratio of TUNEL-positive cells/total number of cells counted (at least 1000 cells).

Statistical Analysis

For diabetic disease onset, logistic regression was used to examine the effect of EGCG. Terms for group (EGCG vs. water), time (8 weeks, 16 weeks, 22 weeks), and the interaction between group and time were considered for possible inclusion in the model using both backward elimination and forward selection. Under backward elimination, both main effects and their interaction were forced into the logistic regression model. Since an interaction should not be included in a model unless both main effects are present, the interaction term was then tested to determine if it should be dropped from the model by comparing the deviance for the saturated model (consisting of both main effects and their interaction) with the deviance for the reduced model (consisting of only the main effects). A non-significant test result indicated that the interaction term should be dropped. If the interaction term was dropped, each main effect was tested in turn to determine if either of them should be dropped. The process continued until no terms could be dropped without significantly affecting the fit of the model. In the forward selection process, each main effect term was added in turn, and the deviance for a model with

one predictor was compared with the deviance for the model with no predictors. The process continued until there were no additional significant effects to be added to the model. Every test in both model-building procedures was based on a difference of deviances, all of which have approximate χ^2 distributions with degrees of freedom corresponding to the difference in degrees of freedom for the competing models. Each of these tests was performed at the 0.05 level of statistical significance.

For the lymphocytic infiltration area calculation, we compared the "water" and EGCG-treated groups using statistical methods that take into account the fact that the number of lymphocytes was measured three times by BIOQUANT software for each animal in each group. A separate comparison of the groups was performed at each time point so that we could assess changes over time in the differences between the groups in terms of number of lymphocytes.

For other assay results, ANOVA and two tailed student t-test were used to analyze the samples with either SEM or SD presented in the results. Values with $p<0.05$ is considered statistically significant between treatment groups.

Results

Diabetic disease onset

We chose to give the animals EGCG by bottle-feeding ad libitum instead of other methods such as gavage or injection, to avoid stress-induced autoimmune disease onset. Female NOD mice develop diabetes beginning at week 12 of age (Jackson Laboratories, 2007 Diabetes Incidence study data for Stock No. 001976). At 8 weeks of age, animals appeared normal without signs of stress, weighing 17.8 to 23.2 grams. There was no urine glucose detected in any animal group. At 16 weeks of age, 8 out of 12 animals in the water-fed group, and 3 out of 12 animals in the EGCG-fed group, tested positive for urine glucose. Three EGCG-fed animals lost weight, although they did not test positive for urine glucose. At 22 weeks of age, only 3 of the 12 animals in the water-fed group remained negative for urine glucose, while 7 of the 12 EGCG-fed animals were negative (Fig 1A).

To calculate this set of data, the backward elimination procedure based on the likelihood ratio (LR) test was applied to determine whether the group and time main effects and the interaction between these two factors should be included in the model. The LR test for retaining the interaction effect was not significant ($\chi^2 = 0.08$, d.f. = 2, $p = 0.961$). Next, both the group and time main effects were tested for elimination. The LR tests for retaining both main effects were significant: group ($\chi^2 = 29.29$, d.f. = 2, $p < 0.001$) and time ($\chi^2 = 7.06$, d.f. = 1, $p = 0.008$). The forward stepwise procedure produced similar results, indicating that "time" should be added to the model first ($\chi^2 = 27.28$, d.f. = 2, $p < 0.001$), followed by group ($\chi^2 = 7.06$, d.f. = 1, $p = 0.008$), and that the group by time interaction should not be added ($\chi^2 = 0.08$, d.f. = 2, $p = 0.961$). Therefore, only the group and time main effects were included in the final logistic regression model. The significant result for the time factor indicates that there was a significant increase in the rate of onset of diabetes over the course of the study. The significant result for the group factor indicates that there was a significant difference between the group treated with EGCG and the group treated with water in terms of the rate of onset of diabetes, with the EGCG-treated group having a significantly slower rate of onset.

In addition, an odds ratio method was used to assess the data. At 16 weeks of age, the odds for the EGCG-fed mice to be disease-free is almost 6.1 more times than the water-fed mice; at 22 weeks of age, the odds for the EGCG-fed mice to be disease-free is about 4.2 more times compared to the water-fed mice.

The body weights in both groups were normal at 16 weeks of age. At 22 weeks of age, there was no significant difference in body weight average between the groups ($p>0.05$). Within both groups, 2 animals showed a significant decline ($p<0.05$) in body weight relative to the rest of the group. These data show that EGCG in the water did not affect overall food consumption or body weight.

Serum total anti-nuclear antibody level change

At 8 weeks of age, serum total anti-nuclear antibody levels in both groups were at background (optical absorbance of >0.3 is considered positive for total autoantibodies). In the water-fed group, by the age of 16 weeks total serum autoantibody levels were significantly elevated at 0.37±0.13 ($p<0.05$, two tailed t-test). By 22 weeks of age, serum total anti-nuclear antibody levels were 0.424±0.09, but this value was not significantly different from the 16 week value ($p=0.33$). In the EGCG-fed group, by 16 weeks of age, serum total anti-nuclear antibody levels were also significantly increased to 0.34±0.09 ($p<0.01$). By 22 weeks of age, serum total anti-nuclear antibody levels were 0.318±0.038, not significantly higher than that at 16 weeks of age ($p>0.46$) (Fig. 1B). When the two groups are compared, at 22 weeks of age, the total serum autoantibody level in the EGCG-fed group was significantly lower ($p<0.005$) than the level in the water-fed group (Fig 1B). That is, EGCG reduced, but did not entirely prevent, the age-dependent rise in total serum autoantibody levels in the NOD mouse.

Histomorphologic analysis

The morphology of the submandibular glands of EGCG-treated animals was compared to that of water-fed (EGCG-negative) animals of 22 weeks of age. Gross, macroscopic evaluation indicated a significant textual difference between the glands from EGCG and water-fed animals. While glands from EGCG-treated animals exhibited a relatively firm and normal tactile textual consistency on manual palpation immediately following dissection and prior to fixation in formalin, glands from water-fed animals were distinctly soft in textual consistency. Furthermore, histological examination of hematoxylene and eosin (H&E) stained section of gland tissues from both animals under the light microscopic power (20X) showed a distinct enlargement of the acinar and intercalated ducts of glands from the water-fed group compared to glands from EGCG-fed animals (Fig 2A). Glands from water-fed animals also exhibited significant interstitial fibrosis (Fig 2A, arrow). The markedly increased size of the glands from water-fed animals reflects enhanced hypertrophy with or without accompanying hyperplasia. For example, the brush borders of striated ducts of glands from the water-fed animal (2A) appeared much denser than those of glands from EGCG-treated animals (2B).

Lymphocytic infiltration in the submandibular glands

At 8 weeks of age, one out of 12 animals in the water-fed group and three out of 12 in the EGCG-fed group had small lymphocytic infiltrations. There was no statistical difference between the groups in the areas of the lymphocytic infiltrations (999.77 ± 3463.30 vs. 2896.56 ± 3716.60, $p = 0.209$, all results are given as Mean ± SD, ANOVA two-tailed *t* test). In the water-fed group, by 16 weeks of age, the average area of lymphocytic infiltration had increased dramatically to 49757.87 ± 26407.40 ($p<0.0001$). By 22 weeks of age, the average area of lymphocytic infiltration was not increased further (60599.66 ± 40230.24; $p>0.3$). In the EGCG-fed group, by 16 weeks of age, the average area of lymphocytic infiltration had increased to 28639.64 ± 15613.84 ($p<0.0001$). By 22 weeks of age, the average area of lymphocytic infiltration showed a further significant increase (51442.32 ± 31730.66; $p<0.003$). Figure 2 are representative photos from which the lymphocytic infiltrates were quantitatively measured by BIOQUANT software.

When the two treatment groups are compared at 16 weeks of age, the average area of lymphocytic infiltration in the EGCG-fed group was significantly lower ($p=0.026$). By the age

of 22 weeks, there was not significant difference (p=0.599) (Fig 3). That is, EGCG delayed (but did not prevent) the increase in lymphocytic infiltration of the NOD mouse submandibular glands.

Apoptotic activity in the salivary glands

The apoptotic activity was determined by TUNEL staining of the salivary glands (Fig 4A) and quantification (Fig 5A). At 8 weeks of age, apoptotic activity throughout the glandular epithelium was very low in both treatment groups (water-fed 0.11%±0.03; EGCG-fed 0.1% ±0.03). In the water-fed group, at the age of 16 weeks apoptotic activity in the glandular epithelium was increased significantly to 0.15%±0.18 ($p<0.05$). Within the lymphocytic infiltrates, apoptotic activity was substantially higher than in the glandular epithelium (0.41% ±0.15, $p<0.0001$). By 22 weeks of age, apoptotic activity in the glandular epithelium was 0.35% ±0.11, a significant ($p<0.0001$) 2.3-fold increase over the 16 week value. Within the lymphocytic infiltrates, apoptotic activity was more than 9-fold higher than in the glandular epithelium (3.20%+1.10; $p<0.0001$), and nearly 8-fold higher than the 16 week lymphocytic infiltrate value ($p<0.0001$).

In the EGCG-fed group, at the age of 16 weeks apoptotic activity in the glandular epithelium was increased significantly to 0.18%±0.12 ($p<0.05$). Within the lymphocytic infiltrates, apoptotic activity was substantially higher than in the glandular epithelium (1.19%±0.56, $p<0.0001$). By 22 weeks of age, apoptotic activity in the glandular epithelium was 0.36%±0.34, not statistically different than the 16 week value ($p=0.11$). Within the lymphocytic infiltrates, apoptotic activity was 0.87%±0.26, only 2.4-fold higher than in the glandular epithelium ($p<0.003$), and no different to the 16 week lymphocytic infiltrate value ($p=0.13$).

There is no significant difference between the two treatment groups in the levels of apoptotic activity in the glandular epithelium at either 16 or 22 weeks of age ($p>0.38$). For comparison, the level of apoptosis in BALB/c control mice at 22 weeks is 0.1%. However, significant differences between the two groups were seen in apoptotic activity in the lymphocytic infiltrates. At 16 weeks of age, apoptosis in the infiltrates in EGCG-fed mice was 2.9-fold higher that in the water-fed group ($p<0.001$). However, at 22 weeks of age, the level in EGCG-fed mice was unchanged, and 3.7-fold lower that in the water-fed group ($p<0.0001$). That is, EGCG did not affect the modest levels of apoptosis in the glandular epithelium, but did affect apoptosis in the infiltrates, initially raising levels, but blocking the considerable increase seen at 22 weeks in water-fed mice (Fig 5A).

PCNA expression in the submandibular glands

In the water-fed group, PCNA immunostaining (Fig 4B) and quantification (Fig 5B) demonstrated relatively low levels of positive cells in the glandular epithelium at 8 and 16 weeks of age (0.52%±0.57 and 0.32%+0.80, respectively, $p>0.5$). However, by 22 weeks of age, the number of PCNA-positive cells had increased by a remarkable 45-fold compared to 16 weeks of age (14.64%+8.86, $p<0.0001$). In the EGCG-fed group, PCNA levels were low at 8 and 16 weeks of age (0.13%±0.08 and 0.20%±0.25, $p>0.3$). At 22 weeks, PCNA-positive cells had increased to just 1.08%±1.24, only a 5-fold increase compared to 16 weeks of age ($p<0.03$).

When the two groups are compared, even at the early age of 8 weeks, PCNA-positive cells in the EGCG-fed group were 4-fold lower than the water-fed group ($p=0.026$). By 16 weeks of age, PCNA levels were comparable between the groups. However, by 22 weeks of age, PCNA nuclear staining in the water-fed group was more than 13-fold higher than in the EGCG-fed group ($p<0.0004$) (Fig 4B and Fig 5B). In comparison, BALB/c mice at 22 weeks of age showed similar PCNA expression (approximately 1%) to EGCG group.

That is, in water-fed NOD mice, there is a dramatic rise in PCNA-positive cells between 16 and 22 weeks of age, and EGCG considerably reduces this rise and maintains levels comparable to normal control mice. The vast majority of the PCNA-positive cells are localized to the ductal epithelial cells (Fig. 6A). Of these positive cells, most show cytoplasmic staining, but a significant minority show nuclear staining. Some ducts also showed PCNA immunostaining in the lumen (Fig 6A).

Ki-67 expression in the submandibular glands

In the water-fed group, Ki-67 immunostaining (Fig 4C) and quantification (Fig 5C) demonstrated relatively low levels of positive cells in the glandular epithelium at 8 and 16 weeks of age (0.41%+0.41, 0.07%+0.07). The level at 16 weeks of age was 5.8-fold lower than at 8 weeks of age ($p<0.02$), possibly reflecting cessation of animal growth. However, by 22 weeks of age, the number of Ki-67-positive cells had increased by a dramatic 53-fold compared to 16 weeks of age (3.71%+1.96, $p<0.0001$). In the EGCG-fed group, Ki-67 levels were also low at 8 and 16 weeks of age (0.12%+0.18, 0.04%+0.05). As seen in the water-fed group, Ki-67 levels at 16 weeks of age were lower (3-fold) compared to 8 weeks of age, but this difference is not statistically significant ($p>0.16$). At 22 weeks, Ki-67-positive cells had increased nearly 20-fold, to 0.78%±0.53 compared to 16 weeks of age ($p=0.0001$).

As seen in PCNA staining, when the two groups are compared, even at the early age of 8 weeks, Ki-67-positive cells in the EGCG-fed group were 3.4-fold lower than the water-fed group ($p<0.04$). Similarly by 16 weeks of age, Ki-67 levels were comparable between the groups ($p>0.3$). However, by 22 weeks of age, Ki-67 nuclear staining in the water-fed group was nearly 5-fold higher than in the EGCG-fed group ($p=0.0005$) (Fig 4C and Fig 5C). In comparison, BALB/c mice at 22 weeks of age showed similar Ki-67 expression (approximately 0.66%) to the EGCG group.

That is, in NOD mice, Ki-67 levels behaved similarly to PCNA levels and were affected by EGCG in the same way: in the water-fed group, there was a dramatic rise in Ki-67-positive cells between 16 and 22 weeks of age, and EGCG reduces this increase and maintains levels comparable to normal control mice. The proportion of Ki-67-positive cells at 22 weeks of age in the water-fed group was almost a fourth of that of the PCNA-positive cells (3.71% vs. 14.64%). The vast majority of the Ki-67-positive cells are localized to the ductal epithelial cells (Fig. 6B). No significant cytoplasmic staining was seen.

Discussion

It is interesting to notice that there is a differential autoimmune diabetic disease onset time between water-fed and EGCG-fed groups. At week 16 of age, 67% of control mice developed insulin-dependent diabetes, while only 25% of EGCG-fed mice developed insulin-dependent diabetes (n=12). At week 22 of age, 78% of control mice became diabetic, while only 45% of EGCG-fed animals developed insulin-dependent diabetes (n=9). EGCG significantly delayed the onset of diabetes in the animals (Fig 1). This discovery is encouraging and warrants future studies to determine the underlying mechanism.

We previously reported that green tea extract possesses inhibitory effects on lymphocytic infiltration and serum autoantibody production in NOD mice 3 weeks post positive urinary glucose detection (Hsu et al., 2007). The current study showed that EGCG, the most abundant GTP, also has inhibitory effects in lymphocytic infiltration and serum autoantibody production (Fig 1A, Fig 2 and Fig 3). These results indicate that the protective effects of GTPs are, at least in part, contributed by the anti-inflammatory and anti-apoptotic properties of EGCG.

On the other hand, lymphocytic infiltration into the salivary glands is not always associated with positive urinary glucose. Lymphocytic infiltration was detected as early as 8 weeks of age in 17% of the animals (4 of out 24), at which time none of the animals were tested positive for urinary glucose. This observation suggests that the autoimmune reaction that targets the secretory glands was triggered at very early stage, prior to the reproductive age of these animals (8 weeks old), resulting in the migration of lymphocytes into the submandibular glands, and perhaps other secretary glands such as the lacrimal glands and pancreas.

Therefore, it is logical to separate the autoimmune disease progression in NOD mice to three stages: disease triggering (early), disease advancing (midterm), and gland tissue destructing (late). The role of EGCG appears to play in all three stages. EGCG could influence the onset of autoimmune disease in NOD by modulating gene expressions and/or protein activities in the acinar cells (perhaps other cell types too) of secretary glands, resulting in a weakened local autoimmune manifestation and allowing the acinar cells to continue functioning for an extended time. This protective effect led to a delayed onset of diabetes in the NOD mice possibly due to EGCG's presence in the pancreatic tissue, especially the islets of β cells. During the disease advancing stage (week 8 through week 16 of age), the most visible symptom of the autoimmune disease is the lymphocytic infiltration into the secretary glands and positive urinary glucose, while the autoantibody production and apoptotic activity remained relatively low in the salivary glands. At this stage, EGCG consumption was associated with significantly reduced lymphocytic infiltration (Fig 3) and the number of animals with positive urinary glucose (Fig 1A). This protective effect of EGCG during the disease advancing stage may be attributed to the anti-inflammatory property of EGCG that is able to confine the lymphocytic infiltration into the secretory glands, therefore reducing the lymphocytemediated dysfunction of these glands.

However, the autoimmune-induced dysfunction of secretory glands appears not strongly associated with acinar cell apoptosis, since at this disease advancing stage (week 16 of age), acinar cell apoptosis, at least in the submandibular glands, is not significantly increased in any group in comparison to the Balb/c strain (Fig 5A). Thus, we postulate that dysfunction of the secretory glands is due to changes of cellular behavior, such as undifferentiation, proliferation, and cell type conversion, rather than the direct result of lymphocyte-induced apoptosis.

Apoptotic activity in the salivary glands of NOD mice increased significantly at week 22 of age, when the disease progression is in the tissue destruction stage and animal begin to lose weight and die. At this stage, lymphocytic infiltration to the glands became more efficient, overcame the protective effect of EGCG (Fig 3). Thus, the total lymphocytic-infiltrated areas between water-fed and EGCG-fed groups were no longer statistically different, despite EGCG-fed animals had a smaller average lymphocytic area in absolute Bioquant measurement (Fig 2 and Fig 3). On the other hand, EGCG significantly reduced the number of TUNEL-positive cells in the glands (Fig 4A and Fig 5A), and maintained a relatively low autoantibody production (Fig 1B) in comparison to the water-fed animals. It is apparent that increased apoptotic activity in the glands is associated with elevated total serum autoantibody levels as seen in the water-fed animals at week 16 of age. However, the relationship between apoptosis and autoantibody production is still not clear. It is likely that elevated autoantibody levels caused the increased number of apoptotic cells, and this increased apoptotic activity further stimulated the autoantibody production by releasing more autoantigens into the circulation system to form a feedback loop that eventually results in total dysfunction of the glands.

During this stage, a new observation was recorded: a significant high level of proliferating cells in the gland. Both PCNA and Ki-67 immunostaining confirmed this phenomenon (Fig 4B, 4C, Fig 5B, and 5C). These proliferation markers are significantly elevated in the salivary glands of water-fed NOD mice in comparison to the Balb/c mouse glands. Interestingly, the EGCG-

fed animals showed only moderate increase in PCNA and Ki-67 nuclear proliferation markers (Fig 4B and 4C). Histological evaluation also suggest that the salivary glands from the water-fed NOD mice exhibit enlarged acinar and duct structures, and signs of fibrosis (Fig 2A). It is not clear why cell proliferation is associated with the final stage of autoimmune disease progression. It could be explained as stem cell and/or fibroblasts proliferation to replace lost cells in the gland caused by autoimmune-induced cell death. It may also be explained that gland cells are converted from terminally differentiated cells to proliferating cells that are less differentiated. Under either circumstance, these cells have lost the secretory function. This may explain that Sjogren's syndrome-associated xerostomia is not always a consequence of complete acinar cell loss (Jonsson *et al.* 2006).

Ki-67 is specific for proliferating cells, whereas PCNA is expressed during S phase and repair. Many of the PCNA-positive cells showed cytoplasmic localization (Fig 6A). This would account for the higher proportion of PCNA-positive cells as compared to Ki-67-positive cells in the glands of 22 week old water-fed mice. Cytoplasmic localization of PCNA raises the possibility of inappropriate intracellular trafficking. Consistent with this, some ducts showed immunostaining for PCNA in the lumen, suggesting secretion. This could account, in part, for PCNA being targeted as an autoantigen.

The current study indicates that the protective effects of EGCG at this stage were at multiple scales. It maintains the total serum autoantibody production at moderate levels (Fig 1B); inhibits the expression of PCNA and Ki-67 protein levels (Fig 4B, 4C, Fig 5B, and 5C); and suppressed apoptotic activity in the glands (Fig 4A and Fig 5A). We previously reported that EGCG significantly inhibited TNFα-induced apoptosis in human salivary gland acinar cells *in vitro* (Hsu et al., 2007). This inhibitory effect on apoptosis could be due to modulation of MAPK signal to interrupt an apoptotic signal (Hsu et al., 2007). On the other hand, inhibition of cell proliferation by EGCG might be achieved by its pro-differentiation property previously described (Hsu et al., 2003). Finally, the relatively low levels of serum total autoantibodies could be resulted from EGCG's inhibitory effect on autoantigen expression (Hsu et al., 2005).

In conclusion, the most abundant green tea polyphenol EGCG significantly delayed the onset of autoimmune diabetes, effectively protected the salivary gland cells from autoimmune-induced damage at multiple levels. Systemically, EGCG consumption at 0.2% leads to a moderate level of serum total autoantibodies, and resulted in a smaller number of animals developed insulin-dependent diabetes. In the salivary glands, 0.2% EGCG consumption reduced lymphocytic infiltration during the disease advancing stage, inhibited apoptotic activity, and suppressed the expression of cell nuclear proliferation markers PCNA and Ki-67. Taken together, oral consumption of EGCG could provide protective effects in the secretory cells against autoimmune-induced damage, and sustain cellular function in the secretory glands by preventing these highly differentiated cells from signals for proliferation and/or apoptosis. However, the mechanisms for such multi-level protection by EGCG are still poorly understood, which warrant further investigation in order to unveil the working mechanisms of this unique phytochemical for human benefits.

List of abbreviations

GTPPs, green tea polyphenols; EGCG, (-)-epigallocatechin-3-gallate; ROS, reactive oxygen species; NOD, non-obese diabetic.

LITERATURE CITED

Baudouin C, Pisella PJ, Brignole F. Current treatments of xerophthalmia in Sjögren's syndrome. Rev Med Interne 2004;25:376–382. [PubMed: 15110955]

Bolstad AI, Jonsson R. Genetic aspects of Sjögren's syndrome. Arthritis Res 2002;4:353–359. [PubMed: 12453311]

Cassolato SF, Turnbull RS. Xerostomia: clinical aspects and treatment. Gerodontology 2003;20:64–77. [PubMed: 14697016]

Cha S, Peck AB, Humphreys-Beher MG. Progress in understanding autoimmune exocrinopathy using the non-obese diabetic mouse: an update. Crit Rev Oral Biol Med 2002;13:4–16.

Cravens PD, Lipsky PE. Dendritic cells, chemokine receptors and autoimmune inflammatory diseases. Immunol Cell Biol 2002;80:497–505. [PubMed: 12225387]

Fox PC. Salivary enhancement therapies. Caries Res 2004;38:241–246. [PubMed: 15153695]

Fox RI. Sjogren's syndrome: evolving therapies. Expert Opin Investig Drugs 2003;12:247.

Hayashi Y, Arakaki R, Ishimaru N. Apoptosis and estrogen deficiency in primary Sjögren's syndrome. Curr Opin Rheumatol 2004;16:522–526. [PubMed: 15314488]

Hayashi Y, Arakaki R, Ishimaru N. The role of caspase cascade on the development of primary Sjögren's syndrome. J Med Invest 2003;50:32–38. [PubMed: 12630566]

Hsu S, Bollag WB, Lewis J, Huang Q, Singh B, Sharawy M, Yamamoto T, Schuster G. Green tea polyphenols induce differentiation and proliferation in epidermal keratinocytes. J Pharmacol Exp Ther 2003;306:29–34. [PubMed: 12663686]

Hsu S, Dickinson D. Green Tea: A New Approach to Managing Oral manifestations of Sjogren's Syndrome and Skin Manifestations of Lupus. Journal of Biochemistry and Molecular Biology 2006;39:229–239. [PubMed: 16756750]

Hsu S, Dickinson DP, Qin H, Borke J, Ogbureke K, Winger JN, Walsh DS, Bollag WB, Stoppler H, Sharawy M, Schuster G. Green tea polyphenols reduce autoimmune symptoms in a murine model for human Sjogren's syndrome and protect human salivary acinar cells from TNF-alpha-induced cytotoxicity. Autoimmunity 2007;40:138–147. [PubMed: 17364504]

Hsu S, Dickinson D, Qin H, Lapp C, Lapp D, Borke J, Walsh DS, Bollag WB, Stoppler H, Yamamoto T, Osakai T, Schuster G. Inhibition of Autoantigen Expression by (-)-Epigallocatechin-3-Gallate (the Major Constituent of Green Tea) in Normal Human Cells. J Pharmacol Exp Ther 2005;315:805–811. [PubMed: 16046615]

Humphreys-Beher MG, Yamachika S, Yamamoto H, Maeda N, Nakagawa Y, Peck AB, Robinson CP. Salivary gland changes in the NOD mouse model for Sjögren's syndrome: is there a non-immune genetic trigger? Eur J Morphol 1998;36:247–251. [PubMed: 9825931]

Jonsson MV, Delaleu N, Brokstad KA, Berggreen E, Skarstein K. Impaired salivary gland function in NOD mice: association with changes in cytokine profile but not with histopathologic changes in the salivary gland. Arthritis Rheum 2006;54:2300–2305. [PubMed: 16802370]

Khurshudian AV. A pilot study to test the efficacy of oral administration of interferon-alpha lozenges to patients with Sjögren's syndrome. Oral Surg Oral Med Oral Pathol Oral Radiol Endod 2003;95:38–44. [PubMed: 12539025]

Manganelli P, Fietta P. Apoptosis and Sjögren's syndrome. Semin Arthritis Rheum 2003;33:49–65. [PubMed: 12920696]

Morbini P, Manzo A, Caporali R, et al. Multilevel examination of minor salivary gland biopsy for Sjogren's syndrome significantly improves diagnostic performance of AECG classification criteria. Arth Res Ther 2005;7:R343–R348. [PubMed: 15743482]

Mukhtar H, Ahmad N. Tea polyphenols: prevention of cancer and optimizing health. Am J Clin Nutr 2000;71(6 Suppl):1698S–1702S. [PubMed: 10837321]

Ohno S, Suzuki T, Dohi Y. The effect of bakumondo-to on salivary secretion in Sjogren syndrome. Ryumachi 1990;30:10–16. [PubMed: 2377938]

Porter SR, Scully C, Hegarty AM. An update of the etiology and management of xerostomia. Oral Surg Oral Med Oral Pathol Oral Radiol Endod 2004;97:28–46. [PubMed: 14716254]

Rehman HU. Sjögren's syndrome. Yonsei Med J 2003;44:947–954. [PubMed: 14703600]

Rosen A, Casciola-Rosen L. Altered autoantigen structure in Sjögren's syndrome: implications for the pathogenesis of autoimmune tissue damage. Crit Rev Oral Biol Med 2004;15:156–164. [PubMed: 15187033]

Sawalha AH, Potts R, Schmid WR, Scofield RH, Harley JB. The genetics of primary Sjögren's syndrome. Curr Rheumatol Rep 2003;5:324–332. [PubMed: 14531961]

Sueoka N, Suganuma M, Sueoka E, Okabe S, Matsuyama S, Imai K, Nakachi K, Fujiki H. A new function of green tea: prevention of lifestyle-related diseases. Ann N Y Acad Sci 2001;928:274–280. [PubMed: 11795518]

Van Woerkom JM, Geertzema JG, Nikkels PG, Kruize AA, Smeenk RJ, Vroom TM. Expression of Ro/SS-A and La/SS-B determined by immunohistochemistry in healthy, inflamed and autoimmune diseased human tissues: a generalized phenomenon. Clin Exp Rheumatol 2004;22:285–292. [PubMed: 15144121]

Yamamoto K. Pathogenesis of Sjögren's syndrome. Autoimmun Rev 2003;2:13–18. [PubMed: 12848970]

Zhao LJ, Li ZJ, Huang YY, Ti ZK, Chen Y. Experience on 60 cases of Sjögren's syndrome diagnosed and treated with traditional Chinese medicine. J Tradit Chin Med 1989;9:31–34. [PubMed: 2761281]

Acknowledgment

The authors thank Ms. Vera B. Larke for her technical assistance.

This study was supported in part by funds from a grant from MCG, a fund from US Army Periodontics, and from Department of Oral Biology, School of Dentistry to S.H.

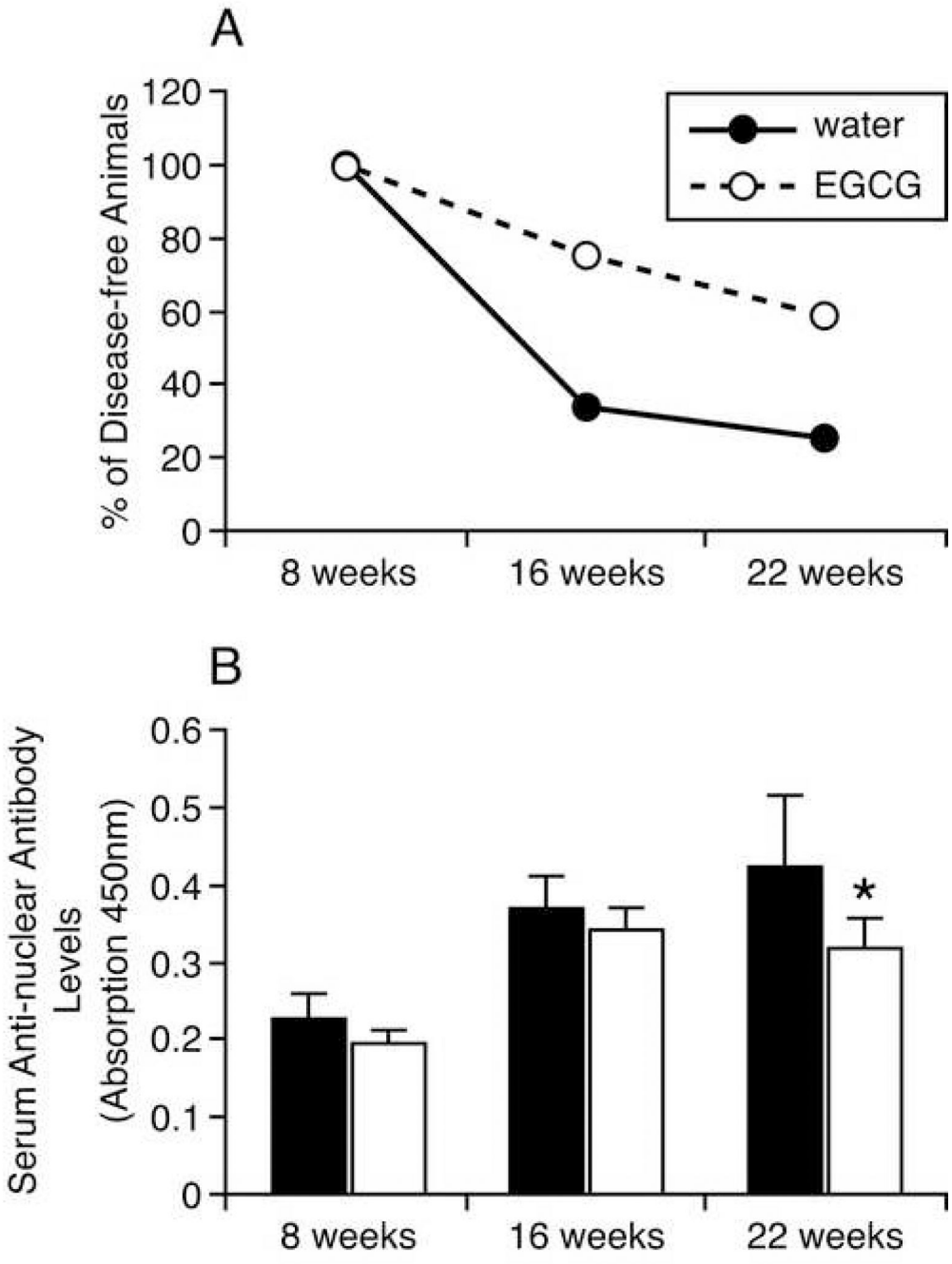

Figure 1.

A. Diabetes disease onset detected by urinary glucose test. There was no urine glucose detected in any animal group at the age of 8 weeks. At 16 weeks of age, 8 animals in the water-fed group tested positive for urine glucose; 3 animals in the EGCG-fed group were positive. At 22 weeks of age, only 3 out of 12 animals in the water-fed group were negative for urine glucose, while 7 out of 12 in the EGCG-fed animals were negative. **B. Total serum anti-nuclear antibody determination by ELISA**. Serum total anti-nuclear antibody concentration in each NOD mouse was measured by the Mouse Anti-Nuclear Antibodies (ANA) ELISA Kit at the age of 8 (n=12), 16 (n=10) and 22 weeks (n=9). Values of each bar represent absorption measurements for each group. Y-error bars represent SEM. At the age of 22 weeks, serum total

anti-nuclear antibody levels are significantly lower in EGCG-fed animals than water-fed animals (two-tailed student *t-test* analysis, $p<0.005$).

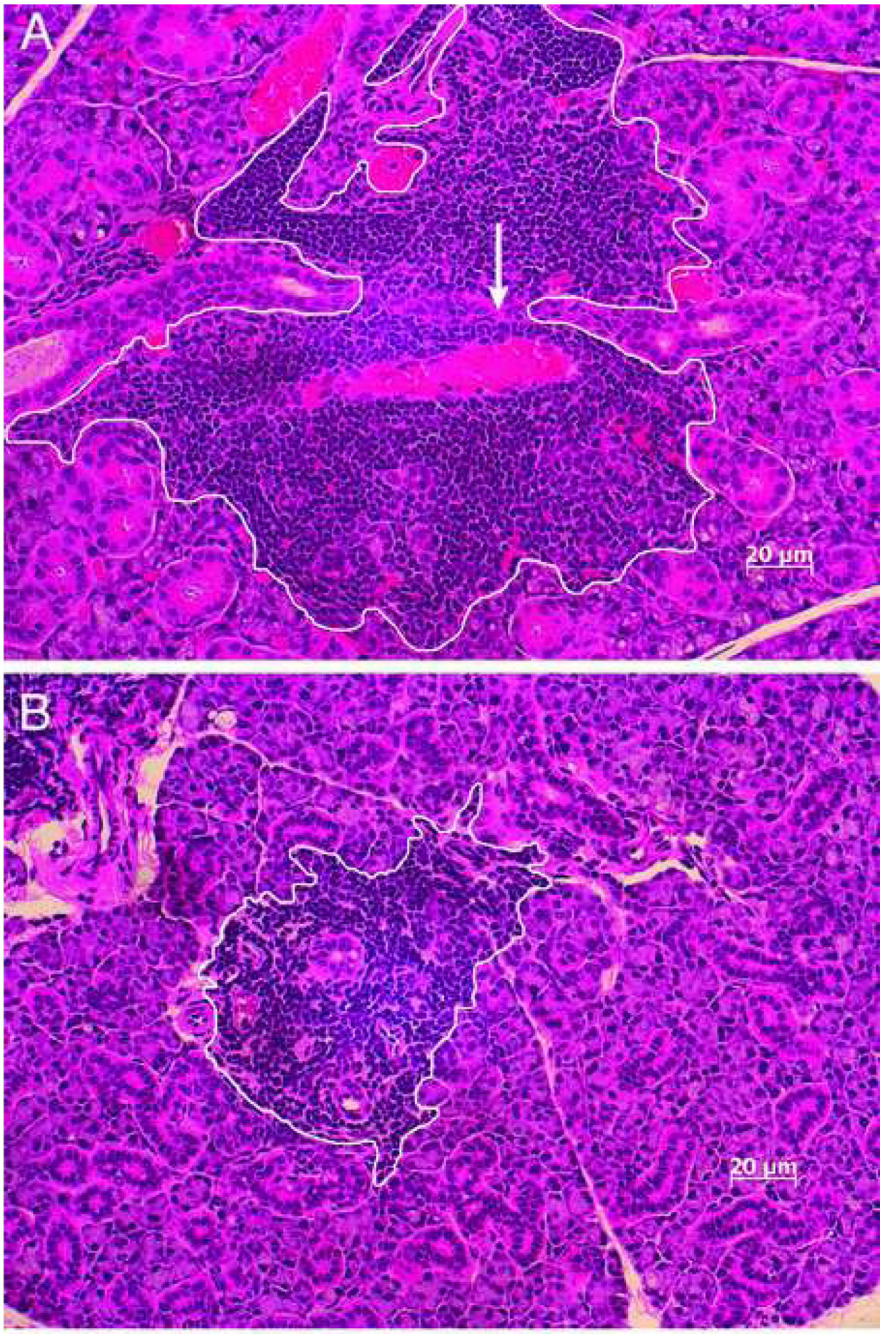

Figure 2.

Representative H&E stained submandibular gland sections of water-fed (left) and EGCG-fed (right) NOD mice (20X). Histological examination of hematoxylene and eosin (H&E) stained section of gland tissues from water-fed and EGCG-fed animal groups at 22 weeks of age demonstrates a distinct enlargement of the acinar and intercalated ducts of glands from the water-fed group (A) compared to glands from EGCG-fed animals (B). Glands from water-fed animals also exhibited significant interstitial fibrosis (arrow). White lines encircle the areas of lymphocytic infiltration measured by BIOQUANT NOVA PRIME 6.75 software.

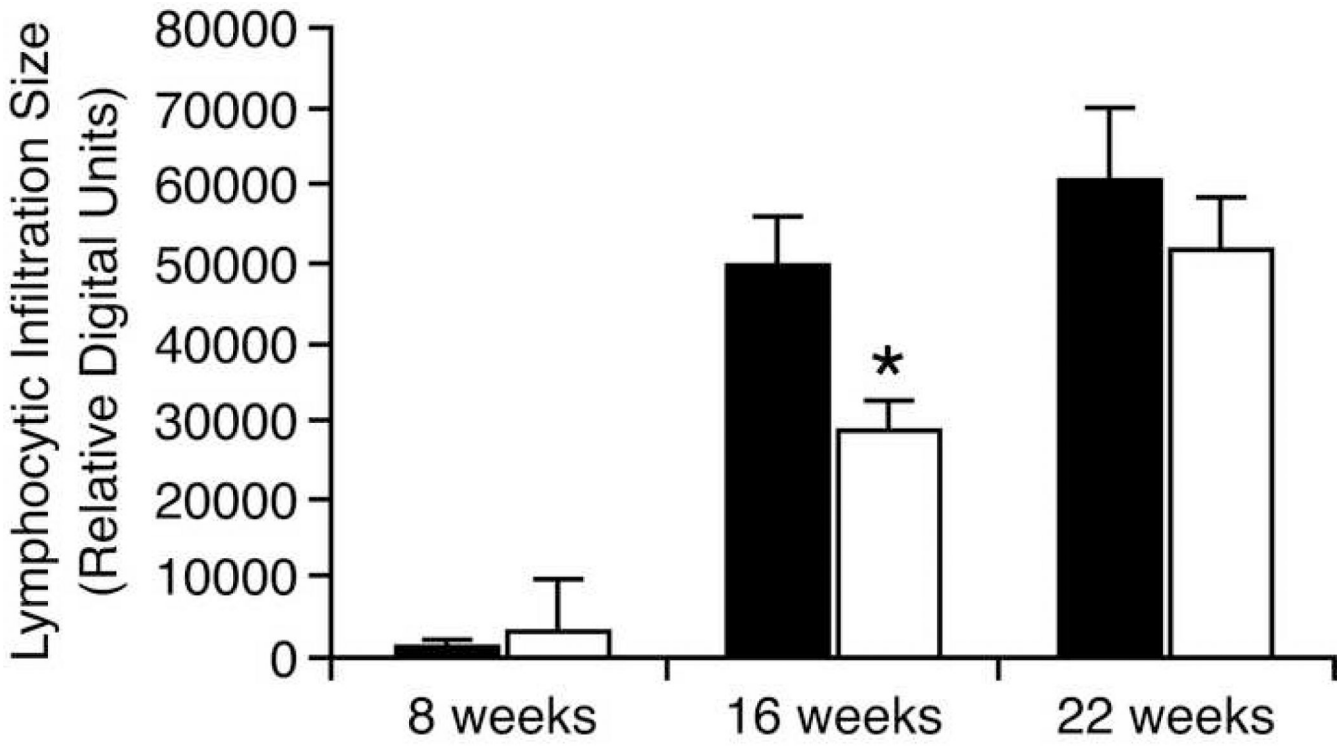

Figure 3.

Average focal areas of submandibular gland lymphocyte infiltration in NOD mice at different age. Animals were fed either with EGCG/water or water only. At the age of 8 (n=36), 16 (n=36) and 22 weeks (n=27), submandibular glands were dissected, processed and stained by H&E. Three randomly selected areas of lymphocytic infiltrates were measured in each gland as relative density units generated by BIOQUANT NOVA PRIME 6.75 software, representing area sizes. Error bars are standard error of means (SEM). Results were analyzed by the two-tailed t-test analysis. * At 16 weeks of age, the average lymphocytic infiltrated area in EGCG-fed animals is significantly lower that in water-fed animals (p=0.026).

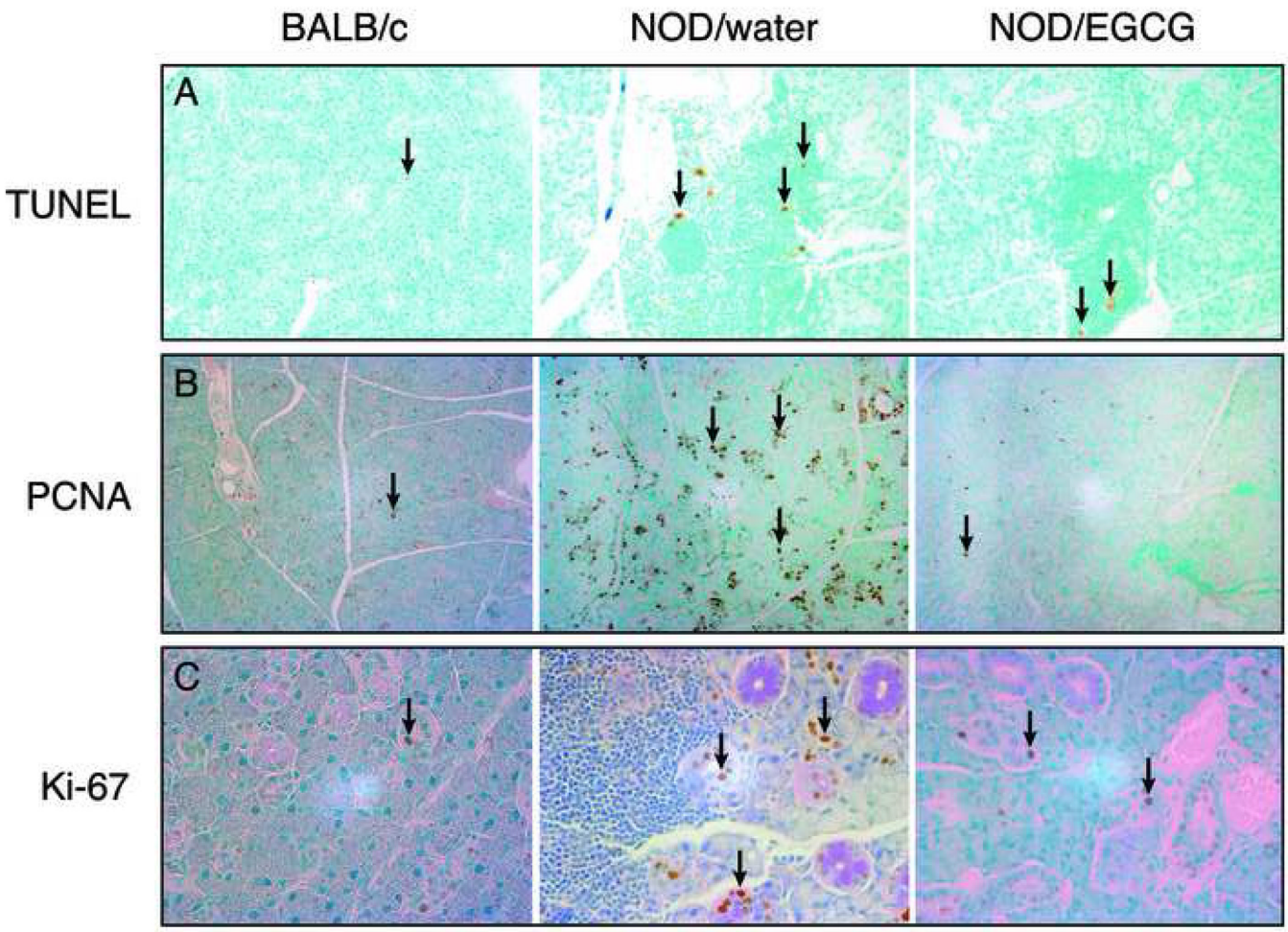

Figure 4.

A. Representative TUNEL staining of submandibular glands from BALB/c, water-fed, and EGCG-fed NOD mice at 22 weeks of age (magnification 10X). Submandibular salivary gland samples from BALB/c (left), water-fed (middle), and EGCG-fed (right) NOD mice were stained with ApopTag Plus Peroxidase *in situ* apoptosis detection method according to the manufacturer's instructions. Red arrows point to the nuclear staining of TUNEL-positive cells. **B. Representative PCNA immunostaining of submandibular glands from BALB/c, water-fed, and EGCG-fed NOD mice at 22 weeks of age (magnification 10X)**. Submandibular salivary gland samples from BALB/c (left), water-fed (middle), and EGCG-fed (right) NOD mice were immunostained with the anti-PCNA antibody. Red arrows point to the nuclear staining of PCNA-positive cells. **C. Representative Ki-67 immunostaining of submandibular glands of BALB/c, water-fed, and EGCG-fed NOD mice at 22 weeks of age (magnification 40X)**. Submandibular salivary gland samples from BALB/c (left), water-fed (middle), and EGCG-fed (right) NOD mice were immunostained with the anti-Ki-67 antibody. Arrows point to the nuclear staining of Ki-67-positive cells.

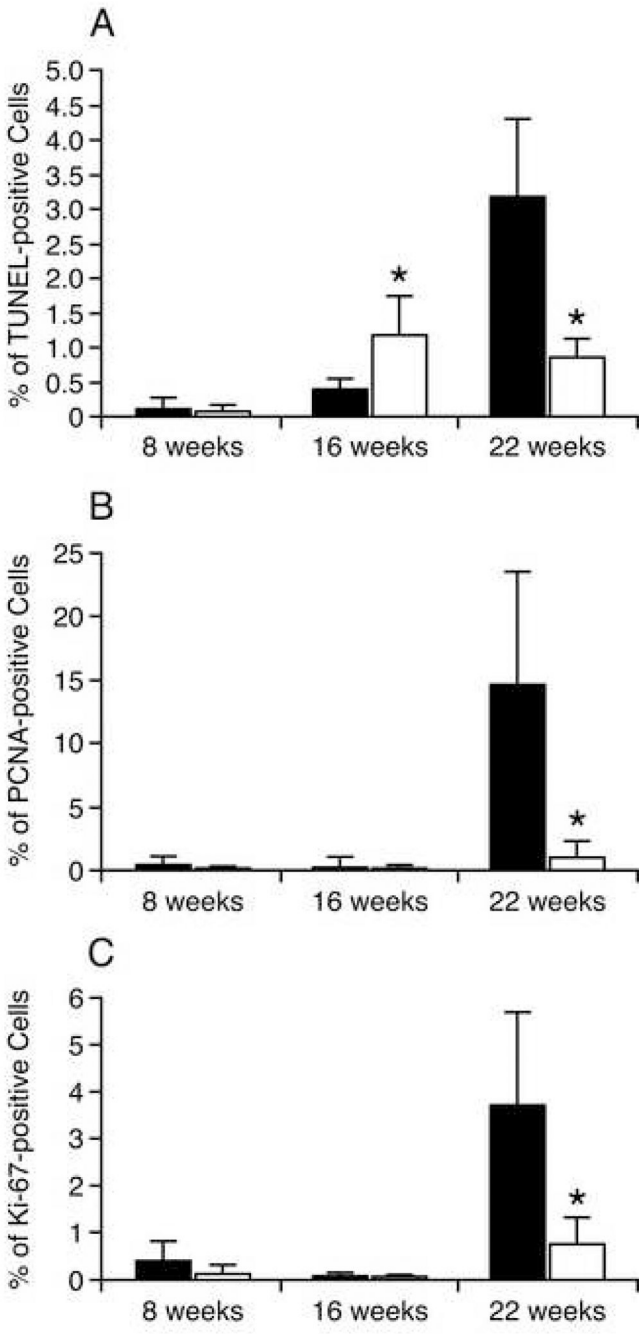

Figure 5.

A. Percentage of TUNEL-positive cells in the submandibular gland epithelium of water-fed and EGCG-fed NOD mice at 8, 16, and 22 weeks of age. Solid bars represent the average percentage of TUNEL-positive cells in the submandibular gland of water-fed NOD mice. Open bars represent the average of TUNEL-positive cells in the submandibular gland of EGCG-fed NOD mice. **B. Percentage of PCNA-positive cells in the submandibular gland epithelium of water-fed and EGCG-fed NOD mice at 8, 16, and 22 weeks of age**. Solid bars represent the average percentage of PCNA-positive cells in the submandibular gland of water-fed NOD mice. Open bars represent the average of PCNA-positive cells in the submandibular gland of EGCG-fed NOD mice. **C. Percentage of Ki-67-positive cells in the submandibular gland**

epithelium of water-fed and EGCG-fed NOD mice at 8, 16, and 22 weeks of age. Solid bars represent the average of Ki-67-positive cells in the submandibular gland of water-fed NOD mice. Open bars represent the average of Ki-67-positive cells in the submandibular gland of EGCG-fed NOD mice. * Statistical difference was found between the two treatment groups. y-error bars represent SD.

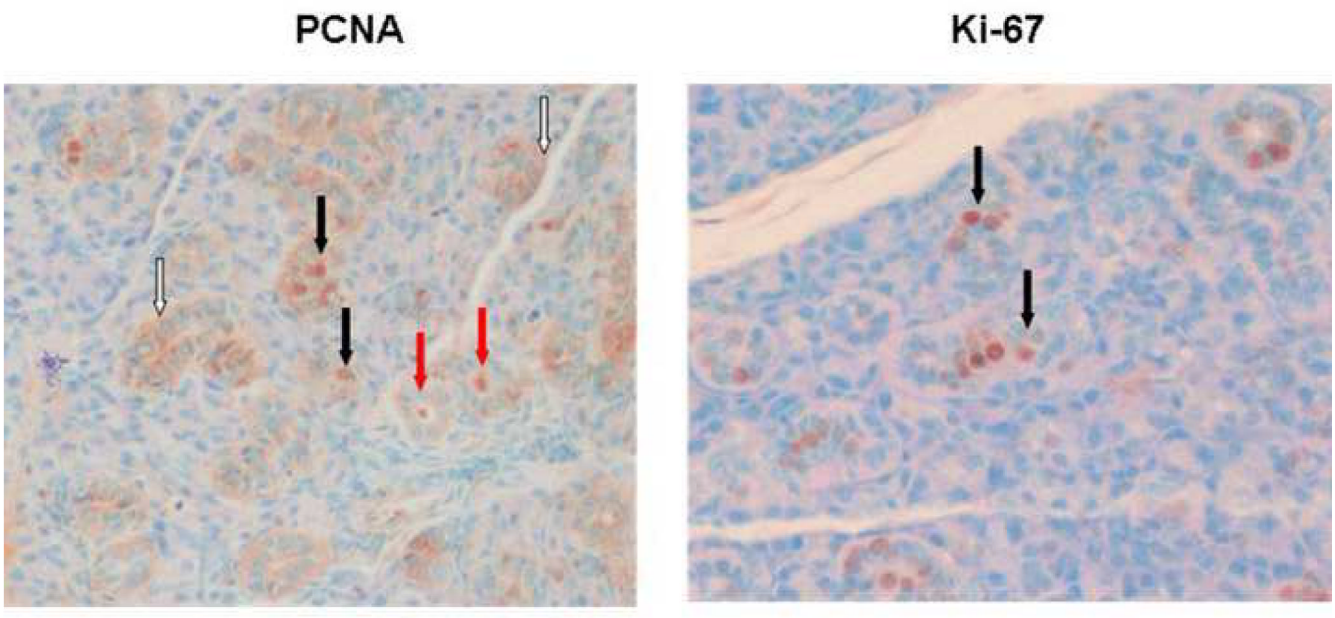

Figure 6.

PCNA and Ki-67 expression in glandular epithelium of 22 week old water-fed animals (magnification 40X). A. PCNA immunostaining.Solid arrows point to representative nuclear staining of ductal cells; open arrows to areas of cytoplasmic staining; red arrows to PCNA immunostaining in the lumen of some ducts. **B. Ki-67 immunostaining**. Solid arrows point to representative nuclear staining of ductal cells.